SYNTHESIS AND CHARACTERIZATION OF NANOSTRUCTURED ZINC OXIDE (ZnO) FOR SENSOR APPLICATIONS

By

HIND I. ABDULGAFOUR

Thesis submitted in fulfillment of the requirements for the degree of Doctor of philosophy

June 2013

ACKNOWLEDGEMENTS

On this memorable night in my life when I am going to finish the writing of this thesis, first of all I bestowed the thanks to Allah Almighty for granting me health with capability to complete this research work. I dedicated this thesis to the soul of my father and mothers, God have mercy on them. Along the way to the completion of this thesis, my family, my husband, my son Taha, sisters, and my brother all contributed in different ways. At this moment I am very thankful to all of them.

I would like to express my deep sense of gratitude to my supervisor, Prof. Zainuriah Hassan for her useful and valuable suggestions, inspiring guidance and consistent encouragement without which this thesis could have never been materialized. She always taught me how to face hard moments in this research.

I also wish to record my sincere thanks to my co-supervisor, Dr. Yam Fong Kwong for his kind cooperation, valuable contribution, patience and guidance during my study and research work.

To be fair I had to extend my sincere thanks to all of NOR lab staff for the cooperation and kindness behaviors with all the postgraduate students. I also thank all my friends and colleagues who supported me and helped me at the School of Physics, Universiti Sains Malaysia.

TABLE OF CONTENTS

LIST OF TABLES

LIST OF FIGURES

LIST OF SYMBOLS

a	Lattice constant
a_o	Bohr radius
A	Area
A^{**}	Richardson's constant
Λ_{air}	The thickness of the space-charge layer
c	Lattice constant
d	Interplanar spacing of the crystal planes
D	Average crystal size
e	Charge of electron
φ_B	The potential barrier
E_C	Conduction band
E_F	Fermi level of semiconductor
E_g	Semiconductor band gap
E_g^{bulk}	The bulk energy of ZnO
$E_g^{nano}(a)$	Infinite potential barriers
E_v	Valence band edge
E_w	The effective barrier height
F	Force
h	Planck's constant
$(hkil)$	Mille indices
I	Current
I_o	Saturation current
J	Current density
k	Boltzmann constant
m_o	Electron mass
m^*	Effective mass
m_n	Electron effective mass
m_p	Hole effective mass
Nc	Effective density of states
N_D	Donor concentration
N_A	Acceptor concentration
NWs	Nanowires
n	Ideality factor
q	Electron charge
R	Responsivity
R_s	Series resistance
S	Sensitivity
t	Thickness
T	Absolute temperature
V	Voltage
V_d	Diffusion voltage
ΔV	Electrical polarization
w	Width
α	Absorption coefficient
ε	Permittivity
ε_o	Absolute dielectric constant
ν	Frequency

θ_i	Hydrogen atoms coverage at the interface
θ	Incident / Diffraction angle
χ_S	Semiconductor electron affinity
φ_B	Schottky barrier height
ϕ_m	Metal work function
ϕ_S	Semiconductor work function
μ_e	Electron mobility
μ	Carrier mobility
ω	Photon frequency
λ	Wavelength
η	Quantum efficiency
β	Contrast ratio of photo and dark current

LIST OF MAJOR ABBREVIATIONS

ALE	Atomic layer epitaxy
a.u.	Arbitrary unit
BL	Blue luminescence
C	Crystal-field split band
CB	Conduction band
CBD	Chemical bath deposition
CMOS	Complementary metal-oxide semiconductor
CVD	Chemical vapour deposition
CVT	Chemical vapour transport
1D	One dimensional
3D	Three dimensional
DBE	Donor bound exciton
DC	Direct current
DLE	Deep level emission band
DOS	Density of state
ECD	Electrochemical deposition
EDX	Energy dispersive X-ray
eV	Electron volt
FE	Field Emission
FWHM	Full width at half maximum
HCP	Hexagonal close packing
HVPE	Hydride vapour phase epitaxy
HWE	Hot-wall epitaxy
I-V	Current-Voltage
LA	Longitudinal-acoustic
LCVD	Laser chemical vapour deposition
LD	Laser diode
LDA	Local density approximation
LED	Light emitting diode
LPCVD	Low-pressure chemical vapour deposition
LPE	Liquid phase epitaxy
LO	Longitudinal optical
M	Metal
MBE	Molecular beam epitaxy
MOCVD	Metalorganic chemical vapour deposition
MOSFET	Metal-oxide semiconductor field effect transistors
MS	Metal-semiconductor
MSM	Metal semiconductor metal
PECVD	Plasma enhanced
PVT	Physical vapour transport
PL	Photoluminescence
PLD	Pulsed laser deposition
PS/Si	Porous silicon substrate
QDs	Quantum dots
QWs	Quantum wells
RL	Red luminescence
rms	Root mean square
SBH	Schottky barrier height

sccm	Standard cubic centimeters per minute
SEM	Scanning electron microscope
SPE	Solid-phase epitaxy
TA	Transverse-acoustic
TEM	Transmission electron microscopy
TFE	Thermionic field emission
TLM	Transmission line model
TO	Transverse optical
UHV	Ultra high vacuum
UV	Ultra Violet
UST	Ultrasonic treatment
VB	Valence-band
VLS	Vapour-liquid-solid mechanism
VPE	Vapour-phase epitaxy
VS	Vapour-solid mechanism
XRD	X-ray Diffraction
YL	Yellow luminescence
WZ	Wurtzite structure
ZB	Zinc blend structure

SINTESIS DAN PENCIRIAN STRUKTUR NANO ZINK OKSIDA (ZnO) UNTUK APLIKASI PENDERIA

ABSTRAK

Projek ini memberi tumpuan kepada pembangunan pendekatan baru untuk menumbuh pelbagai struktur nano ZnO berkualiti tinggi tanpa pemangkin melalui kaedah kos rendah dengan penyejatan haba basah untuk aplikasi penderia. Pertumbuhan struktur nano dan mikro ZnO adalah dengan pengoksidaan basah serbuk Zn melalui mekanisme wap pepejal (VS). Dalam bahagian pertama kerja ini, kesan suhu yang berbeza bagi sintesis struktur nano ZnO yang berkualiti tinggi pada substrat Si/SiO_2 telah dikaji. Suhu pertumbuhan boleh dibahagikan kepada tiga kawasan: rendah (550-650˚C), sederhana (700-800˚C), dan tinggi (850-900˚C). Fabrikasi struktur nano ZnO berkualiti tinggi untuk aplikasi penderia dihadkan dalam kawasan suhu sederhana ke suhu tinggi. Kesan tempoh yang berbeza ke atas pertumbuhan rod nano ZnO juga dibincangkan. Selain daripada itu, fabrikasi struktur mikro dan struktur nano 3-dimensi (3D) ZnO yang baru pada suhu yang berbeza dalam satu langkah tanpa pemangkin telah ditunjukkan. Ciri-ciri struktur dan optik serta mekanisme pertumbuhan pelbagai struktur nano ZnO telah disiasat dan dicadangkan. Prestasi terbaik peranti untuk rod nano ZnO berupa tetrapod yang tumbuh pada Si/SiO_2 telah difabrikasikan untuk mengkaji kesan suhu penyepuhlindapan haba pada sifat elektrik Pd/ZnO rod nano berupa tetrapod. Peningkatan masa sambutan foto Pd/ZnO rod nano berupa tetrapod yang berkos rendah untuk pengesanan ultraungu (UV) telah diperolehi. Didapati bahawa sambutan maksimum fotopengesan Pd/ZnO logam-semikonduktor-logam (MSM) adalah 0.106 A/W pada 300 nm yang bersepadanan dengan kecekapan kuantum sebanyak 43.8 % pada 5 V voltan pincang yang dikenakan.

Dalam bahagian kedua, satu kajian perbandingan pengesan UV berdasarkan hasil tinggi struktur nano ZnO yang berbeza telah dijalankan iaitu dengan menggunakan rod nano yang berjajar dengan baik (atas Si (100)), dawai nano berupa rambut (atas silikon berliang (PS)), dan rod nano berupa tetrapod (atas kuarza). Kajian ini telah menunjukkan bahawa dawai nano ZnO/PS mempamerkan sambutan foto yang agak cepat, dengan masa naik sebanyak 0.089 s dan masa susut sebanyak 0.085 s berbanding dengan struktur nano atas substrat lain. Dalam bahagian ketiga, kesan substrat iaitu PS dan Si ke atas penumbuhan struktur nano ZnO telah disiasat. Kajian menunjukkan bahawa bentuk baru struktur nano ZnO yang berupa terumbu karang telah diperolehi atas substrat PS, dan juga, rod nano ZnO seperti bunga yang berjajar telah dihasilkan atas substrat Si. Morfologi kasar permukaan PS adalah berfaedah untuk pertumbuhan struktur nano dimana saiz bijian boleh dikurangkan dan bilangan tapak penukleusan boleh ditingkatkan. Seterusnya, satu kajian perbandingan sifat-sifat pengesanan hidrogen berdasarkan struktur nano Pd/ZnO atas substrat Si dan PS telah dilakukan. Kepekaan dan suhu operasi optimum bagi penderia tersebut adalah 350% (pada 100˚C) untuk ZnO/PS pada 150 sccm gas H_2, adalah lebih daripada dua kali kepekaan maksimum untuk peranti ZnO/Si pada 150˚C.

Dalam bahagian terakhir, peranti dengan rekabentuk baru 2-dalam-1 telah ditunjukkan; peranti ini terdiri daripada struktur MSM untuk pengesanan gas dan simpang p-n untuk pengesanan UV. Dalam kajian ini, penderia gas MSM Pd/ ZnO/Pd telah berjaya difabrikasikan berdasarkan struktur nano ZnO berupa tiub heksagon. Kepekaan yang tinggi pada suhu bilik penderia ZnO/p-GaN didapati sebanyak 1250% pada 150 sccm gas H_2. Di samping itu, simpang hetero n-ZnO/p-GaN telah berjaya ditunjukkan sebagai fotodiod UV.

SYNTHESIS AND CHARACTERIZATION OF NANOSTRUCTURED ZINC OXIDE (ZnO) FOR SENSOR APPLICATIONS

ABSTRACT

This project focuses on the development of new approach to grow a variety of high quality ZnO nanostructures without catalyst through a low cost method by wet thermal evaporation for sensor applications. The growth of ZnO nano- and microstructures is by wet oxidation of Zn powder via the vapour–solid (VS) mechanism. In the first part of this work, the effect of different temperatures on synthesizing high quality ZnO nanostructures on Si/SiO_2 substrate was studied. The growth temperatures could be divided into three regions: low (550-650˚C), moderate (700-800˚C), and high (850-900˚C), respectively. The fabrication of high quality ZnO nanostructures for sensor applications was confined in the moderate to high temperature regions. The influence of different durations on the growth of ZnO nanorods was also discussed. Apart from that, a novel fabrication of 3D ZnO microstructures and nanostructures at different temperatures in one step without catalyst was presented. The structural and optical properties as well as the growth mechanisms of various ZnO nanostructures have been investigated and proposed. The best performance device for ZnO tetrapod-like nanorods grown on Si/SiO_2 was fabricated to study the effect of thermal annealing temperatures on the electrical properties of Pd/ZnO tetrapod-like nanorods. The enhancement of the photoresponse time of low cost Pd/ZnO tetrapod-like nanorods for ultraviolet (UV) detection was obtained. It was found that the maximum responsivity of the Pd/ZnO metal-semiconductor-metal (MSM) photodetector was 0.106 A/W at 300 nm which corresponds to a quantum efficiency of 43.8% at 5 V applied bias voltage.

In the second part, a comparative study of UV detector based on a high yield of different ZnO nanostructures were carried out i.e. using well-aligned nanorods (on Si (100)), hair-like nanowires (on porous silicon (PS)), and tetrapod-like nanorods (on quartz). The study demonstrated that ZnO nanowires/PS exhibited a relatively fast photoresponse, with a rise time of 0.089 s and fall time of 0.085 s as compared to nanostructures on other substrates. In the third part, the effect of substrates i.e. PS and Si on the ZnO nanostructures was investigated. The study revealed that new shapes of coral reef-like ZnO nanostructures were obtained on PS substrate as well as, flower-like aligned ZnO nanorods were produced on Si substrate. The rough morphology of the PS surface was advantageous for the growth of nanostructures in which the grain size can be reduced and the number of nucleation sites can be increased. Subsequently, a comparative study of hydrogen-sensing properties based on Pd/ZnO nanostructures on Si and PS substrates was performed. The sensitivity and the optimal operating temperature of the sensors are 350% (at 100˚C) for ZnO/PS at 150 sccm of H_2 gas, which is more than twice the maximum sensitivity for the ZnO/Si device at 150˚C.

In the final part, a device with novel 2-in-1 design has been demonstrated; this device consists of MSM structures for gas sensing and p-n junction for UV detection. In this work, a Pd/ZnO/Pd MSM gas sensor has been successfully fabricated based on the nanostructured hexagonal tube-like ZnO. The high sensitivity at room temperature of the ZnO/p-GaN sensor was found to be 1250% at 150 sccm of H_2 gas. In addition, n-ZnO/p-GaN heterojunction has been successfully demonstrated as a UV photodiode.

CHAPTER 1

INTRODUCTION

1.0 The history and current development of ZnO nanostructures

Nanotechnology has been an exciting and rapidly expanding area of research for more than a decade (Morkoc et al., 1994; Krishnamoorthy & Goossen, 1998; Janata, 1992). Studies on the preparation, structure, and properties of nanostructures have been carried out with collective efforts that cross borders between many areas of physical sciences, engineering and biological sciences (Xia et al., 2003).

Studying one dimensional (1D) materials has become a leading edge in nanoscience and nanotechnology. Nanowire-like structures are the ideal system for studying the transport process in one-dimensionally (1D) confined objects; this is important not only for understanding the fundamentals in low dimensional systems, but also for developing a new generation of nanodevices with high performance (Wang, 2004a). With these technological advances, it is possible to make artificial nanometer systems where the effects of the quantum confinement in two dimensions can be observed (2D as in quantum wells), in one (1D as in wires and tubes), and in zero dimension (0D) as in the case of a dot (Dresselhaus et al., 2001; Yoffe, 2001; Yu et al., 1996).

The term "nanostructured material" commonly referred to those materials whose structural element-clusters, crystallites or molecules with one of their physical dimensions is within 1 to 100 nm range. However, there are other definitions of nanostructures in which the physical dimension could be more than 100 nm (Thomas, 2010). It should be noted that the definition of nanostructures with dimension within 100 nm is not strictly followed. According to many research

groups (Peter & Peidong, 2006; Feng et al., 2010; Cho et al., 2008; Thomas, 2010), a wire with diameter from 10 to 200 nm and length around 1-50 μm, a rod with diameter range of 100–600 nm and the length of the nanorods is about several micrometers, a hexagonal tube or disk with diameter about 600 nm and thickness of 200 nm, and a ring with a diameter of 5 μm and a thickness of 300 nm have been studied and they are termed as "nanostructure".

Nanostructured optoelectronic and electronic devices have attracted much interest due to improved device performance in comparison with their non-nanostructures counterparts. For instance, low temperature sensitivity, high differential gain and high modulation bandwidth can be obtained with infrared semiconductor laser when quantum dot layer is used as an active layer (Liu et al., 2001). A Si photoconductive photodetector with nanostructured grating in the active region has shown high responsivity, higher internal quantum efficiency and faster photoresponse (Sharma et al., 2001). In addition, miniaturized single nanowire devices are building blocks for the integrated electronics and photonics of the next generation.

The emergence of nanoscience and nanotechnology, semiconductor nanomaterials have been of great interest due to their unique and novel properties compared with bulk materials (Tang & Kotov, 2005; Comini et al., 2009). Much attention was paid on wide band gap semiconductors in the past decade; and the growth material characteristics of semiconductors with wide band gaps have also been studied with the aim of developing short-wavelength electronic devices based on ZnO, GaN, GaAs, TiO_2, ZnSe and other compounds due to the increasing need for several applications (Wang, 2008).

Zinc oxide, with the formula ZnO, is an inorganic compound which is present in the earth's crust as the mineral zincite (Klingshirn, 2007). It is not a novel material for scientific study, and has been widely used in industry. ZnO can be found in numerous materials and products as an additive including plastics, ceramics, glass, cement, rubber, paint, adhesives, sealants and pigments (Lide, 2001).

As a semiconductor material, ZnO was first studied as early as the 1930s (Bunn, 1935), and the research has focused on bulk ZnO growth, characterizations and applications had rapidly grown since then. By the end of the twentieth century, ZnO had been widely used in the semiconductor industry as varistors operated at elevated temperatures or high voltages (Clarke, 1999), and as ultrasonic transducers in high-frequency regions (Wasa et al., 2004).

From the mid-1990s, ZnO was again under the scientific spotlight. At that time, the initial reason that researchers started to pay attention to this material, was to develop high quality, closely lattice matched substrate materials for GaN which had been viewed as a promising wide band-gap material for short wavelength photonic applications, such as UV and blue light emitting diode (LED) and lasers (Strite & Morkoc, 1992). However, along with the deeper research, it was found that ZnO itself is an excellent wide band-gap material, and can produce bright blue to UV light and laser, which opened a new era for ZnO material (Look et al., 1998; Reynolds et al., 1996; Look et al., 1999). Since then numerous efforts have been devoted worldwide in the research for the realization of ZnO based photonic and optoelectronic devices.

Among the group of II-VI compound semiconductors nanomaterials, ZnO has so far received intense attention due to its remarkable combination of physical and optical properties. ZnO has several important advantages. Firstly, ZnO exhibits both

semiconducting and piezoelectric properties which can be applied in nanogenerators and nanopiezotronics for converting mechanical energy into electrical energy and also for fabricating piezoelectric semiconducting coupled devices (Khan, & Kordesch, 2008). Secondly, ZnO is a direct wide band gap (3.37 eV) semiconductor material with excitation binding energy (60meV) larger than other semiconductor materials such as GaN (25meV) and ZnSe (22meV) (Hsueh, et al., 2006). Therefore, ZnO has attracted much attention as a promising material for solar cells, gas sensor, field emission blue and ultraviolet (UV) light-emitting diodes, and ultraviolet laser devices (Law et al., 2005; Lee et al., 2002; Ryu et al., 2006). Thirdly, ZnO is a biocompatible material that can be used in biochemical and biomedical applications (Nie et al., 2006). Finally, ZnO exhibits the richest range of morphologies among the wide band gap semiconductors owing to its hexagonal wurtzite structure and polar crystal surfaces (Wang, 2004a). A high saturation velocity has been predicted to be ~ 3×10^7 cm/s, potentially leading to fast electronic devices. ZnO has a large photoconductivity, making it suitable for UV photodetectors (Liu et al., 2000; Liang et al., 2001).

The high exciton binding energy in ZnO crystal ensures efficient excitonic emission at room temperature. Ultraviolet (UV) luminescence has been reported in disordered nanoparticles and thin films (Hughes & Wang, 2005). ZnO is transparent to visible light and can be made highly conductive by doping. As a consequence, ZnO is recognized as a promising photonic material in the blue–UV region. As the research on ZnO went deep, increasingly interesting properties and potential applications have been discovered for this material. One of the most attractive aspects is that it is relatively simple for ZnO to form various nanostructures including highly ordered nanowire arrays, tower-like structures, nanorods, nanobelts,

nanosprings and nanorings (Wang, 2006a). Due to the special physical and chemical properties derived from the nanostructures, ZnO has been found to be promising in many other applications, such as for sensing, catalysis, photovoltaics, and nano-generators (Heo et al., 2004a; Schmidt-Mende, & MacManus-Driscoll, 2007; Zou et al., 2009; Law et al., 2005; Wang et al., 2007). The number of articles published on ZnO is on the rise. For example, in 2007 ZnO became the second most popular semiconductor material after Si and that its popularity is still increasing over time (Klason et al., 2008).

The high performance of the nanostructures has kept researchers interested in the synthesis, characterization, and fabrication of nanodevices. As a consequence, many techniques such as molecular beam epitaxy (MBE), chemical vapour deposition (CVD), thermal evaporation, electrodeposition, and sol-gel synthesis have been developed to synthesize nano-structures; sometimes with well controlled size, shape and spatial distribution on the substrates (Heo et al., 2002; Li et al., 2007; Wang, 2004a). On the other hand, rare studies on the synthesis of ZnO nanostructures by wet thermal evaporation method without catalyst have been reported (Han, & Gao, 2009; Chen, et al., 2011).

The synthesis of ZnO nano and microstructures using wet thermal evaporation method without catalyst at different conditions and substrates are required. The simplicity, lower cost, faster growth and suitability of this method to produce variety of nanostructures are very promising for sensor applications. The renewed interest in this material has arisen out of the development of growth technologies for the fabrication of high quality single crystals and epitaxial layers for ZnO-based electronic and optoelectronic devices.

1.1 Statement of the problem

ZnO nanostructures are usually grown by using three zone furnace under vacuum at high temperature under vapour liquid solid (VLS) mechanism (950-1400˚C) with catalyst such as Au, Ni, Pd, and C by thermal evaporation technique (Wang, 2004a). Also, in the VLS mechanism, the catalysts play an essential role in forming liquid alloy; however, this technique needs very high growth temperatures, so that Zn vapor can be dissolved into a metal catalyst to form an alloy droplet. After saturation, Zn precipitates out from the droplet and is oxidized as ZnO nanostructures. Another drawback of the VLS method is that, at the tips of the ZnO nanorods or nanowires, there are always impure metal particles that will lead to contamination, and so these nanostructures are not useful for device fabrication (Sekar et al., 2005).

Apart from that, different solution-based synthesis methods for ZnO nanostructures have been reported (Djurisic, et al, 2010). Solution-based deposition methods can be classified as hydrothermal, solvothermal, and electrodeposition. Hydrothermal method has been widely used to grow ZnO nanostructures on a variety of substrates, and their properties, similar to vapor deposition, have been strongly affected by the seed layer, as well as the substrate orientation and substrate treatment (Djurisic, et al, 2010).

For optical properties, nanostructures prepared by solution methods typically exhibit yellow–orange luminescence, and a large number of structural defects. UV-to-visible emission ratio was dependent on the deposition temperature, and the quality of the seed layer. Significant improvements in the UV-to-visible emission ratios have been observed by both H_2O_2 treatments of as-grown rods, as well as treatment of the catalyst layer (Djurisic, et al, 2010). Regardless of the role and

position of the metal particle during the nanowire growth, it will obviously affect the performance of the optoelectronic devices made using such nanowire arrays, especially if the metal particle is located at the interface of ZnO nanowire and semiconducting substrate. Thus, there is an obvious interest in the fabrication of ZnO nanorod and nanowire without the use of a metal catalyst (Djurisic, et al, 2010).

In this work, growth of ZnO nanostructures were accomplished by using the simplest technique via one stage zone furnace without vacuum at wide range of temperatures from 550˚C to 900˚C and without catalyst. Up to now, few studies have been reported on the subject of catalyst-free fabrication of ZnO such nanowire, tetrapods and nanorod arrays for sensor application. Therefore, growth method without catalyst becomes an important research subject in nanotechnology.

1.2 Objectives of the Study

The aim goal of this research is development on the growth and characterization of a wide range of nanostructured ZnO by using wet thermal evaporation method without catalyst. Simplicity, lower cost, and suitability of this method to produce high structural and optical quality of ZnO nanostructures are very promising for efficient sensor applications such as UV detectors, gas sensors, and p-n heterojunction devices. The objectives of this work can be summarized below:

1. To study the influences of different temperatures in synthesizing ZnO nanostructures in three regions: low (550-650˚C), moderate (700-800˚C), and high (850-900˚C) temperatures. The effects of various experimental parameters on the synthesized ZnO nano- and micro-structures are investigated. The best device for ZnO/Si tetrapod-like nanorods will be

fabricated to study the effect of thermal annealing temperatures on the electrical properties of this device.

2. To study and compare the characterization of UV detectors based on ZnO nanostructures grown on different substrates. The nanostructures will be synthesized on Si (100), porous silicon (PS/Si), and quartz substrates for comparison.
3. To study the effect of the surface roughness of the substrate i.e. PS and Si on the morphological, structural, and optical properties of ZnO nanostructures.
4. To investigate the properties and novel device application of nanostructured hexagonal tube-like ZnO on p-GaN heterojunction.

1.3 Originality of the study

In this work, an alternative method to synthesise of new shapes of high quality ZnO nano and microstructures on Si/SiO_2 such as nanowires, nanorods, nanotetrapods, nanoflowers, pyramid (with nanowires), and micro-sphere (with nanowire) using wet thermal evaporation method without catalyst at different conditions have been accomplished. Currently, the growth of wide range of ZnO nanostructures by thermal evaporation method is an uncontrollable technique (Chen et al., 2011). In this study, the controlled growths of ZnO nanowires at low temperatures as well as aligned ZnO nanorods at different durations have been obtained. The controlled growth was obtained by fixing the growth temperature.

Porous silicon (PS) technology has been utilized to grow new shape of coral reef-like ZnO nanostructures on the surface of Si substrates with rough morphology. Flower-like aligned ZnO nanorods are also fabricated directly onto the silicon substrates through zinc powder evaporation using a simple thermal evaporation method without catalyst for first comparison study between ZnO/PS and ZnO/Si.

This non-catalyst growth technique on the rough surface of substrates may have good potential applications in the fabrication for UV detector and H_2 gas sensor devices.

The first comparative studies of UV detectors based on ZnO nanostructures grown on different substrates are obtained. Pd/ZnO/Pd metal-semiconductor-metal photodetectors have been successfully fabricated using a variety of high-quality ZnO nanostructures. The nanostructures used included well-aligned nanorods, tetrapod-like nanorods, and hair-like nanowires and were synthesized on Si (100), porous silicon (PS/Si), and quartz substrates, respectively, using a catalyst-free vapour–solid mechanism for comparison.

A 2-in-1 device fabricated based on nanostructured hexagonal tube-like ZnO grown on p-GaN heterojunctions works as a gas sensor and UV detector has been achieved.

1. 4 Outlines of the thesis

This thesis consists of eight chapters and is organized as in the following sequence:

Chapter one is the introduction chapter which provides the history, background, and future development of ZnO nanostructures and its applications for some optoelectronic devices.

Chapter two reviews the relevant literature and the basic properties of the ZnO nanostructures, including the crystal structure, electronic and optical characters. The typical synthesis methods of ZnO nanostructures and the advantages of those methods are briefly discussed. A description of the basic principles of the wet thermal evaporation technique is also introduced. The most common substrates that

are used for synthesis of ZnO nanostructures are presented. Finally, some potential applications of ZnO are discussed.

Chapter three describes the relevant theories in this study. A brief explanation of the quantum confinement in semiconductors and the effect of quantum confinement in the nanostructures are explained. The fundamental theory of growth of ZnO nanostructures in wet thermal oxidation process, and the fundamental theories for metal-semiconductor contacts and the basic principles of some devices, which have been fabricated in this project such as metal semiconductor-metal (MSM) photodetector, p-n heterostructures photodiode, and gas sensor are briefly described in this chapter.

Chapter four briefly explains the samples preparation of the ZnO nanostructures with various conditions. Also, the general instruments that were used in this study for characterizations are described. The fabrication and characterization of various types of devices based on ZnO nanostructures are also presented in this chapter.

Chapter five includes the results of synthesis and characterizations of ZnO nanostructures by wet thermal oxidation method are discussed. The growth mechanisms of ZnO nanostructures are also studied based on the experimental results.

Chapter six discusses the results obtained from the synthesis and characterization of ZnO nanostructures grown on different substrates by the wet thermal oxidation method.

Chapter seven is focusing on the study of the performance of the various types of devices fabricated based on ZnO nanostructures.

Chapter eight deals with the conclusions and future works.

CHAPTER2

LITERATURE REVIEW

2.0 Introduction

In this chapter, relevant literature review such as wide-bandgap II-IV semiconductor's properties and growth techniques, semiconductor nanotechnology, and an overview of ZnO nanostructures technology are presented. Apart from that, an overview of the fundamental properties of ZnO nanostructures, growth techniques for ZnO nanostructures and the common substrates used to synthesise ZnO nanostructures are also presented. In addition, the principal applications of ZnO nanostructures will be discussed in detail.

2.1 Wide-bandgap semiconductors and growth techniques

Power semiconductor devices made from materials with bandgap energy larger than in Si (1.12 eV) have been touted for many decades. The potential advantages of these wide-bandgap devices include higher achievable junction temperatures and thinner drift regions because of the associated higher critical electric field values that result in much lower on-resistance than is possible in Si (Chow et al., 1994; Bhatnagar & Baliga, 1993).

Wide-bandgap II–VI compounds are expected to be one of the most vital materials for high-performance optoelectronics devices such as light-emitting diodes (LEDs) and laser diodes (LDs) operating in the blue or ultraviolet spectral range. Additionally, the high ionicity of these compounds makes them good candidates for high electro-optical and electromechanical coupling (Jifeng, & Minoru, 2007).

More research efforts have been invested to study nanostructures-based on wide band gap semiconductors, such as silicon carbide (SiC), gallium nitride (GaN)

and zinc oxide (ZnO) which have been evidenced by a number of publications in this field (Li et al., 2002a; Chiou, 2008; Sun et al., 2008a). Wide-bandgap semiconductor nanostructures have attracted enormous attention due to their unique properties resulted from their low dimensionality. Furthermore, many advantages are provided by the intrinsic nature of wide band gap semiconductors (Hudgins, 2003). Functional oxides of wide band gap semiconductors can be fabricated to form several types of novel nanostructures. These nanostructures are the fundamental building blocks of smart devices. Many metal oxide materials such as ZnO, SnO_2, In_2O_3, Ga_2O_3 and PbO_2 have been investigated and synthesised.

Wide-bandgap II–VI compounds have been applied to optoelectronic devices, because of their direct gap and suitable bandgap energy. Many methods have been extensively applied to grow high-quality thin films and bulk single crystals. Thin films were commonly grown using the conventional vapour-phase epitaxy (VPE) method. As a result of the advancement in science and technology, novel epitaxial growth techniques were developed, including liquid phase epitaxy (LPE), solid-phase epitaxy (SPE), hot-wall epitaxy (HWE), metalorganic chemical vapour deposition (MOCVD), molecular-beam epitaxy (MBE), metalorganic molecular-beam epitaxy (MOMBE) and atomic layer epitaxy (ALE) (Lopez et al., 1978; Manasevit et al., 1971; Chang et al., 1975; Veuhoff et al., 1981; Suntola, 1989). By using these growth methods, film thickness can be controlled, and quality can be improved.

On the other hand, basic research work on growing bulk crystals of wide-bandgap II–VI compounds have been carried out. The focus was on high-quality, and large single crystals (Wang et al., 2001; Song et al., 2003). Since the electrical and optical properties of semiconductor compounds are profoundly affected by impurities and native defects, purity and quality are very important for fundamental research

and engineering application where they are used as substrates. Bulk single crystals of these wide-bandgap II–VI compounds have been grown by the vapour, liquid and solid phases. Vapour-phase growth includes chemical vapour transport (CVT) and physical vapour transport (PVT) methods. Growth methods for films and bulk crystals of wide-bandgap II–VI compounds are summarized in Figure 2.1. This figure is outlined through the literature in this respect with some modifications (Jifeng, & Minoru, 2007).

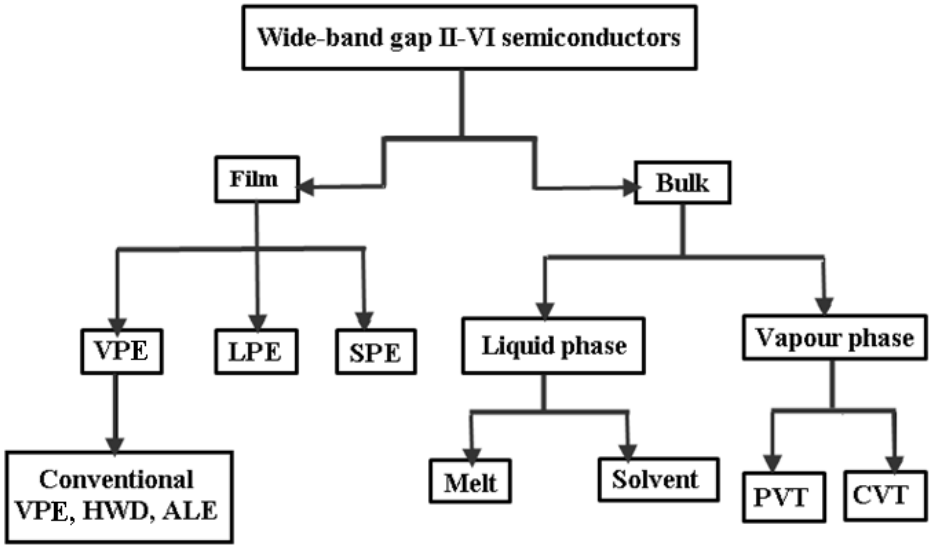

Figure 2.1: Film and bulk-crystal growth techniques for II–VI wide-bandgap compounds [adopted and modified from Jifeng, & Minoru, 2007].

2.2 Overview of semiconductor nanotechnology

Semiconductors are deemed the cornerstone of the modern electronics industry. They have been used extensively in communication, information and computer industries since the invention of semiconductor transistors. During the 2nd half of the twentieth century, miniaturization of semiconductor devices has been adopted so as to increase integration, enhance functionality, and reduce energy consumption. As a result, semiconductor devices have evolved from millimeter-sized

devices capable of manipulating electric currents into micrometer-sized devices that can handle both electricity and light. Another challenge started in the twenty-first century by creating nanometer-sized semiconductor devices that can directly interact with individual atoms and molecules at the nanometer level (Steiner, 2004; Manasreh, 2005; Zurauskiene et al., 2003).

Esaki and Tsu proposed the use of superlattices to observe negative differential resistance (Esaki & Tsu, 1970). They added that advanced epitaxial growth techniques, such as molecular beam epitaxy and metalorganic chemical vapor deposition have been especially developed to enable the growth of high-quality semiconductor alloys under precisely controlled conditions. Impressive progress in the fabrication of low-dimensional semiconductor structures made it possible to reduce the effective dimension from three dimensional bulk materials to quasi-two dimensional quantum well systems, to quasi-one dimensional quantum wires, and even to quasi-zero dimensional quantum dots.

Introduction of quantum wells in the early 1970s was a turning point in the direction of research on electronic structures (Dingle et al., 1974). A quantum well is a very thin layer of a semiconductor sandwiched between two layers of another semiconductor with wider energy gaps.

In the 1980s, the interest of researchers shifted toward structures with further reduced dimensionality such as quantum wires with one-dimensional confinement and quantum dots (QDs) with zero-dimensional confinement (Petroff et al.,1982). The localization of carriers in all three dimensions breaks down the classical band structure of the continuous dispersion of energy as a function of momentum. Unlike quantum wells and quantum wires, the energy level structure of quantum dots is rather discrete. The study of nanostructures has opened a new chapter both in

fundamental physics as artificial atoms and in potential applications as devices (Trojanek et al., 2006; Van & Hannaford, 2005).

2.3 Overview of ZnO nanotechnology

As particles approach the nanoscale, they possess two important properties, the quantum confinement effect and a large ratio of surface area to volume relative to bulk materials (Triboulet & Perriere, 2003). In a bulk crystal, the properties of the material are independent of the size and are only chemical composition-dependent. As the size of a crystal decreases to the nanometer regime, the size of the particle begins to modify the properties of the crystal. In other words, due to the quantum confinement effect, the energy bandgap of nanostructured materials increases with decreasing size of the quantum structures.The large surface area provides numerous atomic sites for the adsorption of molecules, making the nanoparticles attractive materials for gas and chemical sensing. Because nanoparticles are tiny compared to IR and visible wavelengths, they exhibit characteristic absorption and scattering properties (Saraf et al., 2007). This feature has been utilized for materials such as stained glass for many centuries.

The advent of one-dimensional (1D) wide band-gap metal-oxide semiconductors has caused a large billowy effect not only on electronics, but also on photophysics and photochemistry. Research interest in ZnO, one of the wide band gap semiconductors, has waxed and waned over the years. ZnO is one of the few dominant nanomaterials for nanotechnology. ZnO has an effective electron mass of $0.24m_e$, and a large exciton binding energy of 60 meV. Thus bulk ZnO has a small exciton Bohr radius in a range of 1.8-2.3 nm (Wong & Searson, 1999; Gil & Kavokin, 2002; Senger & Bajaj, 2003). Therefore, the quantum confinement effect in ZnO nanowires should be observable at the scale of an exciton Bohr radius. An

example is the well-width dependent PL blue shift which has been observed in ZnO/MgZnO (MQW) epitaxial nanorods with the ZnO well-widths ranging from 1 to 5 nm. Quantum size effect also causes a blue shift in free excitonic emission in ZnO nanorods with diameters smaller than 10nm, (Ohtomo et al., 1999; Park et al., 2003).

Recently, researchers have been focusing on the preparation of diverse morphologies of ZnO nanostructures such as nanowires, nanorods, nanoneedles, nanobows, nanowalls, nanobridges, nano-tetrapods, nano-multipod, nano-flowers, and nanostars (Umar et al., 2006a; Liu, 2002; Park et al., 2002a; Wu et al., 2002a; Hughes et al., 2005; Lao et al., 2004; Lao et al., 2003; Gao et al., 2004; Wang et al., 2006; Umar et al., 2005; Umar et al., 2006b). Figure 2.2 shows a collection of ZnO nanostructures synthesised by thermal evaporation of solid powders (Wang, 2004a).

A major advantage of ZnO nanostructures, such as nanowires and nanorods, is that they can easily be grown on various substrates. Furthermore, these ZnO nanostructures are easily formed even on cheap substrates such as glass and hence they have a promising potential in the nanotechnology future. Particularly, ZnO nanorods can be advantageous with low density of defects. The growth of defect-free structures are more likely for nanorods in comparison with epilayers because the strain in the nanorods can efficiently be relieved by elastic relaxation at the free lateral surfaces rather than by plastic relaxation. Such nanorods are potentially used for gas sensing applications.

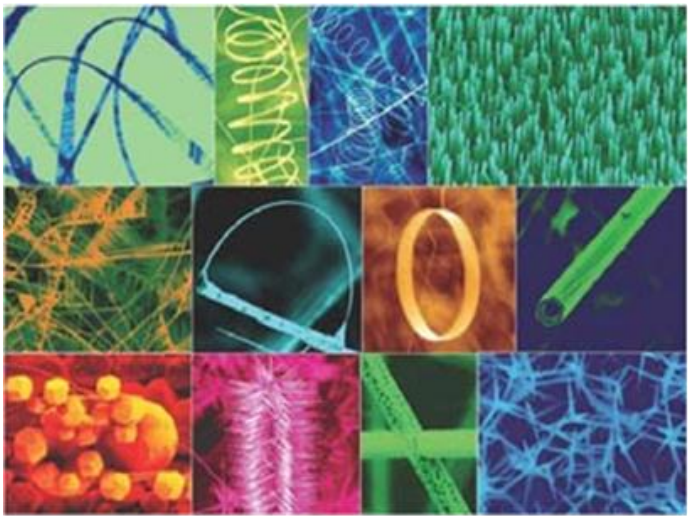

Figure 2.2: A collection of nanostructures of ZnO synthesised under controlled conditions by thermal evaporation of solid powders [adopted from Wang, 2004a].

2.4 Fundamental properties of ZnO

ZnO is grouped under II–VI semiconductors because Zn belongs to group II, and O belongs to group VI in the periodic table. ZnO exhibits the most splendid and abundant configurations of nanostructures that one material can form. Zinc oxide is an inorganic compound which usually appears as a white powder. The chemical bonds that form ZnO are borderline between ionic and covalent bonds though they lean towards being ionic. ZnO has relatively low solubility in water (1.6×10^{-6} g/cm^3 or 2×10^{-6} moles/liter) and even less solubility in ethanol. It decomposes at 1975^{o}C (Florescu et al., 2002).

2.4.1 Crystal structure of ZnO

ZnO crystallizes in three forms: hexagonal wurtzite, cubic zincblende, and the rarely observed cubic rocksalt. The wurtzite structure is the most stable under ambient conditions and thus the most common as shown in Figure 2.3 (a). The zincblende form can be stabilised by growing ZnO on substrates with cubic lattice

structure (Ashrafi et al., 2000; Kim et al., 2003). In both cases, the zinc and oxide centers are tetrahedral. As for the rocksalt (NaCl-type) structure, it is only observed at relatively high pressures about 10 GPa, and cannot be epitaxially stabilised as shown in figure 2.3 (c) (Bates et al., 1962).

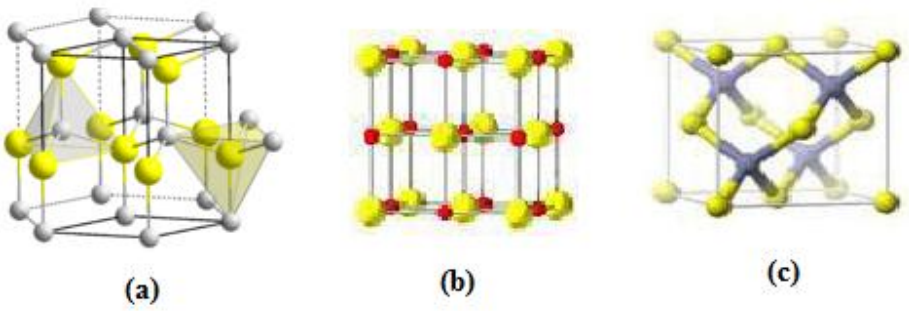

Figure 2.3: (a) The wurtzite structure model of ZnO, (b) the zinc blende, and (c) the rocksalt phases of ZnO [adopted from Bates et al., 1962].

Structurally, ZnO which has a hexagonal crystal structure lattice (space group $C6_{mc}$) which is energetically favorable compared to the rocksalt and zinc blend structures with lattice parameters $a = b = 0.3296$ nm and $c = 0.5206$ nm. The lattice parameters of the unit cell have a c/a ratio of 1.602 which is 1.8% of the ideal hexagonal-close-packed structure of 1.633.

The wurtzite structure of ZnO can simply be described as a number of alternating planes composed of tetrahedrally coordinated Zn^{+2} and O^{-2} ions where each oxygen ion is surrounded tetrahedrally by four zinc ions and vice versa stacked alternately along the c-axis. Another important characteristic of ZnO is polar surfaces. The most common polar surface is the basal plane. The oppositely charged ions produce positively charged $Zn^{+}(0001)$ and negatively charged $O^{-}(000\bar{1})$ surface, resulting in a normal dipole moment and spontaneous polarization along the c-axis as well as a divergence in surface energy.

The polar surfaces generally have facets or exhibit massive surface reconstructions, but ZnO± (0001) are exceptions; they are atomically flat, stable, and without reconstruction (Meyer & Marx, 2003). The other two most commonly observed facets for ZnO are $(2\bar{1}\bar{1}0)$ and $(01\bar{1}0)$, which are non-polar surfaces and have lower energy than the (0001) facets (Wander et al., 2001; Dulub et al., 2003). The interaction among the polar charges at the surface depends on their distribution; therefore the structure is arranged in such a way to minimise the electrostatic energy which is the main driving force for growing polar surface dominated nanostructures.

Together with the polar surfaces due to atomic terminations, ZnO exhibits a large scale of novel structures that can be grown by varying the growth rates along these directions. One of the most important factors determining the morphology involves the relative surface activities of various growth facets under given conditions. Macroscopically, a crystal has different kinetic parameters for different crystal planes which are emphasised under controlled growth conditions. Thus, after an initial period of nucleation and incubation, a crystallite commonly develops to a 3D object with well-defined, low index crystallographic faces. Figure 2.4 (a-d) shows a few typical growth morphologies of one dimensional nanostructures for ZnO (Wang, 2004a). The morphology as shown in Figure 2.4 (d) is dominated by the polar surfaces which can be grown by introducing planar defects parallel to the polar surfaces. Planar defects and twins are observed occasionally parallel to the (0001) plane, but dislocations are rarely seen (Wang, 2004a; Subramanyam et al. 2000). It is observed that when the dimensions of a semiconductor material keep decreasing i.e. from macro to micro to nano scale, some of the physical properties of that material undergo changes. This phenomenon is known as “quantum size effect” (Baruah & Dutta, 2009).

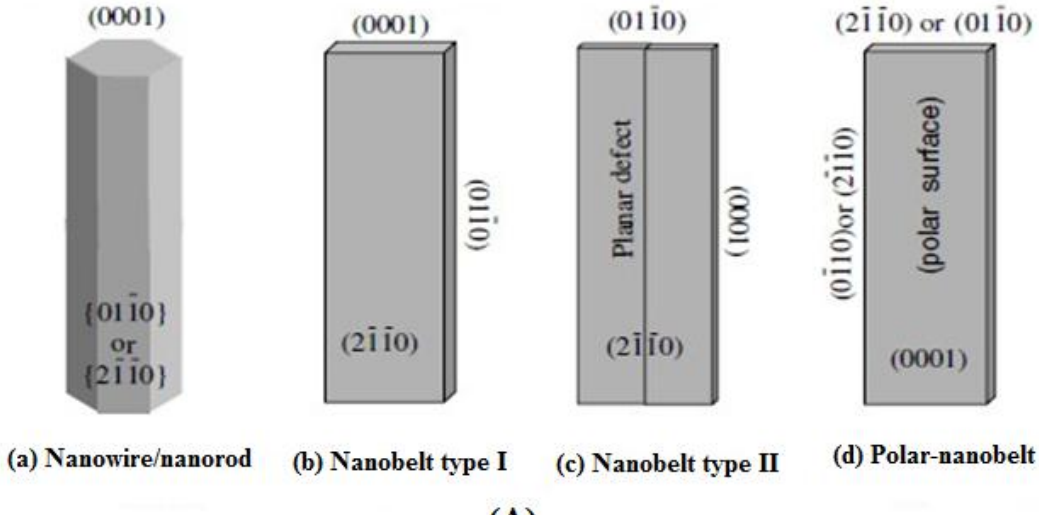

(A)

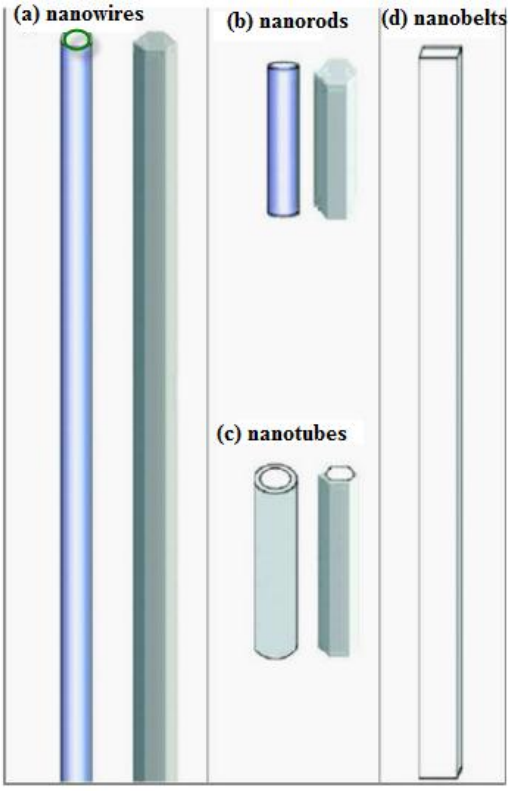

(B)

Figure 2.4: (A) Growth morphology of one dimensional ZnO nanostructures [adopted from Wang, 2004a]. (B) The schematic diagrams of the 1D nanostructures [adopted from Ding & Wang, 2004].

In scientific literature, a few terms are being used for the 1D nanostructures, such as nanowires, nanorods, nanotubes, nanobelts, and nanoribbon. A linear structure with a specific growth direction are usually called nanowires. The side

surfaces and shape of cross-section of a nanowires may not be well defined or uniform shown in Figure 2.4B (a). A nanorod is similar to a nanowire with a shorter length as shown in Figure 4.2B (b). A nanotube is a 1D with a hollow interior chanal (Figure 4.2B (c)). 1D nanostructures with well defined side facets nanobelts/nanoribbons are shown in Figure 4.2B(d), and they have restrictive shape and uniformity than the nanowires.

2.4.2 Physical properties of ZnO

The basic physical properties of ZnO are summarised in Appendix (A) based on the reported data on bulk ZnO at room temperature (Jagadish & Pearton, 2006). There is still uncertainty in the values of the thermal conductivity due to the influence of defects in the material (Florescu 2002). In addition, a stable and reproducible p-type doping in ZnO is still a challenge and cannot be achieved. The findings regarding the values related to the mobility of hole and its effective mass are still arguable. The values of the carrier mobility can surely be enhanced after achieving good control on the defects in the material (Florescu 2002).

2.4.3 Electronic energy bandgap of ZnO

ZnO has a relatively large direct band gap of ~3.37 eV and a relatively large excitation binding energy (60 meV) compared to thermal energy (26meV) at room temperature. Advantages associated with a large band gap include higher breakdown voltages, ability to sustain large electric fields, lower electronic noise, and high-temperature and high-power operation. The electronic band structure of a semiconductor is very important to be understood for its utility in devices and for

further improvement in the performance of these devices (Ozgur et al., 2005). The electronic band structure gives understanding of the electron/hole states.

Several theoretical approaches such as the local density approximation (LDA), the Green's functional method and the first principles were used to calculate the energy band diagram of wurtzite as well as zincblende and rocksalt polytypes of ZnO (Jaffe et al., 2000; Schleife et al., 2006). In parallel to the theoretical efforts, a number of experimental techniques such as X-ray induced photo absorption, photoemission spectroscopy, angle resolved photoelectron spectroscopy, and low energy electron diffraction have commonly been employed to understand the electronic states of wurtzite ZnO (Dong et al., 2004).

The electronic band structure of ZnO has been studied by using local density approximation (LDA) (Vogel et al., 1995) which incorporates atomic self-interaction corrected pseudopotentials (SIC-PP) to accurately estimate the Zn 3d electron. Figure 2.5 shows the band structure diagram reported by Vogel et al., (1995).

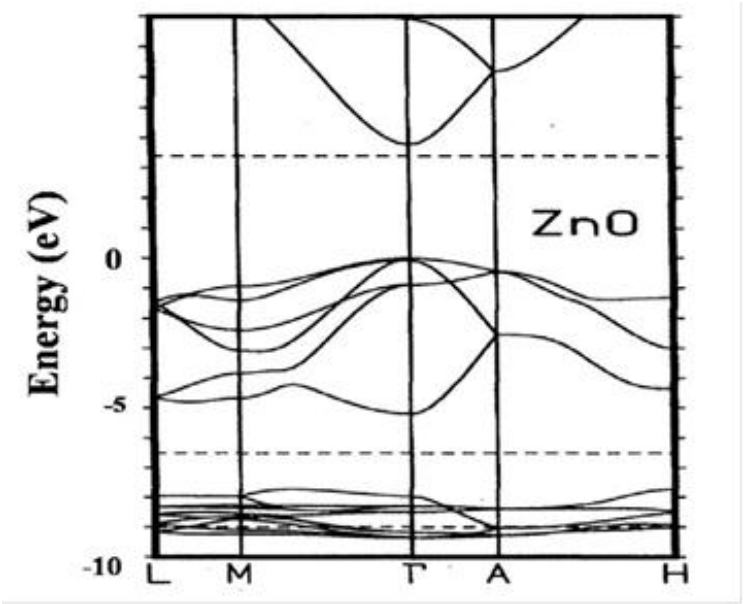

Figure 2.5: LDA band structure of bulk wurtzite ZnO calculated using dominant atomic self-interaction-corrected pseudopotentials (SIC-PP) [adopted from Vogel et al., 1995].

The band structure of ZnO possesses high symmetry lines in the hexagonal Brillouin zone. The direct interband transition takes place between the lowest conduction band and the top of the valence band at the Γ point k=0 in the Brillouin zone. The lowest conduction band of zinc oxide is s-like state having Γ7 (C) symmetry; whereas the valence band is a six-fold that degenerates p-type and is split into three subbands due to spin-orbit interaction and crystal-field effect (Mang et al., 1995). The near band gap intrinsic absorption and emission spectrum is dominated by transitions involving these three valence bands and the conduction band. From the band diagram in Figure 2.5, the bottom 10 bands, which are located at -9eV, correspond to Zn 3d levels. The next 6 bands between -5eV to 0eV correspond to O 2p bonding states. The first two conduction bands are strongly localised and correspond to empty Zn 3s levels. Experimentally, the ZnO valence band is splitted into three band states. The splitting of the valence band as shown in Figure 2.6 where A (heavy hole), B (light hole), and C (crystal-field split band) indicates spin-orbit and crystal-field splitting. A and C subbands are known to possess Γ7 symmetry; while the middle band, B, has Γ9 symmetry.

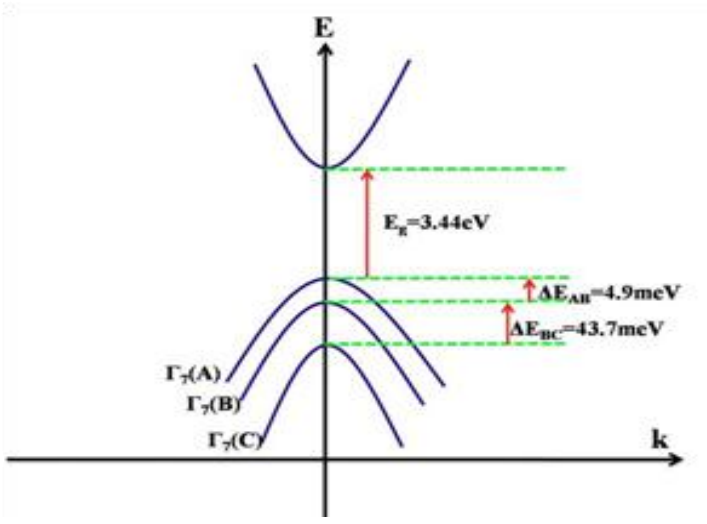

Figure 2.6: Schematic diagram representing the crystal-field and spin-orbit splitting of the valence band of ZnO into 3 subband states A, B, and C at 4.2K [adopted from Jagadish & Pearton, 2006].

2.4.4 Optical properties of ZnO

The optical properties of a semiconductor are dependent on both the intrinsic and the extrinsic defects in the crystal structure. The investigations of the optical properties of ZnO have a long history which started in the 1960s (Thomas, 1960) and recently it has become very attractive among wide band gap materials. The efficient radiative recombinations have made ZnO promising for applications in optoelectronics.

The optical properties of ZnO, bulk and nanostructures, have been investigated extensively by luminescence techniques at low and room temperatures. It is well-known that at room temperature, the PL spectrum of ZnO typically consists of a UV emission band and a broad visible emission band (Vanheusden et al., 1996). The UV emission band is dominated by the free exciton (FE) emission. The broad emission band literally between 420 and 700 nm observed nearly in all the samples regardless of growth conditions is called deep level emission (DLE) band. The UV emission band is related to a near band-edge transition of ZnO, namely, the recombination of the free excitons. The deep level emission band has previously been attributed to several defects in the crystal structure such as O-vacancy (V_O), Zn-vacancy (V_{Zn}), O-interstitial (O_i), Zn-interstitial (Zn_i), and extrinsic impurities (Yamauchi et al., 2004; Yang et al., 2003). Figure 2.7 shows the schematic band diagram of some deep level emissions (DLE) in ZnO.

According to Baruah & Dutta, (2009) and Chen et al., (2004) excitonic emissions have been observed through the PL spectra of ZnO nanorods. It was proved that if we confine the quantum size, then it can greatly enhance the exciton binding energy; furthermore an interesting observation is that the green emission intensity increases with a decrease in the diameter of the nanowires. This is because